


Research Article

Integrated Omics Reveal the Pathogenic Potential of *Blastocystis* sp. ST2

Mengjuan Cao,^{1,2,3} Shaojun Zhang,^{1,2,3} Huizhu Nan,^{1,2,3} Jing Huang,⁴ Chao Zhang,^{1,2,3} Yuxin Sun,^{1,2,3} Liwen Liu,^{1,2,3} Yuping Wang,⁴ Xin Lu,^{1,2,3} and Lei Ma ^{1,2,3}

¹Ministry of Education Key Laboratory of Molecular and Cellular Biology, College of Life Sciences, Hebei Normal University, Shijiazhuang 050024, Hebei Province, China

²Hebei Collaborative Innovation Center for Eco-Environment, Shijiazhuang, Hebei Province, China

³Hebei Key Laboratory of Animal Physiology, Biochemistry and Molecular Biology, College of Life Sciences, Hebei Normal University, Shijiazhuang, Hebei Province, China

⁴Hebei Children's Hospital, Shijiazhuang 050031, China

Correspondence should be addressed to Lei Ma; lmahappy@hebtu.edu.cn

Received 11 October 2023; Revised 12 January 2024; Accepted 1 March 2024; Published 31 March 2024

Academic Editor: Horacio Bach

Copyright © 2024 Mengjuan Cao et al. This is an open access article distributed under the Creative Commons Attribution License, which permits unrestricted use, distribution, and reproduction in any medium, provided the original work is properly cited.

Blastocystis sp. is a zoonotic unicellular eukaryote that is distributed worldwide. The pathogenicity of *Blastocystis* sp. has been debated over the years. In this study, mice were infected with *Blastocystis* sp. ST2 to assess the impact and underlying mechanisms on the host by integrating transcriptomics, metabolomics, and gut microbiomes. Transcriptomic analysis revealed significant differences in the expression of genes related to inflammatory cytokines, tumors, and neuropathic disease-related factors in mice infected with the parasite. A total of 430 differentially expressed genes (DEGs) were identified in *Blastocystis*-infected female mice, as compared with the control mice, and among these genes, the expression levels of 195 were upregulated ($P < 0.001$), and that of 235 were downregulated ($P < 0.001$). Similarly, there were different 478 DEGs in male mice, among which the expression levels of 122 genes ($P < 0.001$) were upregulated, and that of 356 genes were downregulated ($P < 0.001$). Kyoto encyclopedia of genes and genome analysis showed that 22 pathways in females and 28 pathways in males were enriched. Metabolomics results showed obvious metabolite changes in all mice infected with the parasite. In females, 82 different metabolites were identified, among which the expression levels of 27 metabolites were upregulated, and that of 55 metabolites were downregulated. In males, 118 metabolites were identified, among which the expression levels of 24 metabolites were upregulated, and that of 94 metabolites were downregulated. Microbiome analysis showed differences in the richness of bacterial families in *Blastocystis* sp. ST2-infected mice. LEfSe analysis showed differences in the abundance of bacterial families in female and male mice compared to the control groups. Multiomics analysis showed that the transcriptome, metabolome, and microbiome are interrelated. These results emphasize that *Blastocystis* sp. ST2 can negatively affect the host and may be a disease risk factor. The results provide insight into the mechanism of *Blastocystis* sp.–host interactions.

1. Introduction

Blastocystis sp. is a common protistan intestinal parasite found in many animals, including humans [1]. Transmission of *Blastocystis* sp. is believed to occur via animal-to-animal, human-to-human, animal-to-human, and possibly human-to-animal routes [2]. *Blastocystis* sp. has a worldwide distribution with a marked prevalence in many countries. According to most epidemiological studies, nearly all countries of

the world have been classified as well-developed, with a moderate prevalence (10%–15%), or underdeveloped, with a high prevalence (55%–70%). This classification is attributed to the levels of hygiene and the presence or absence of contact with animals and contaminated water and food [3, 4]. After determining *Blastocystis* sp. in water, it has recently been listed as an important indicator for drinking water monitoring by the World Health Organization [5]. *Blastocystis* sp. is genetically diverse, and at least 40 major subtypes have been

identified based on 18S rRNA. Sixteen subtypes, ST1–10, ST12, ST14, ST16, ST23, ST35, and ST41, have been reported in humans, and ST1–4 is the most common in humans, accounting for more than 90% of reports [2, 6, 7]. Due to the influence of the geographical environment and other factors, there are differences in the prevalent subtypes in different regions, and different subtypes may have differences in pathogenicity. This may also be one of the reasons why the pathogenicity of *Blastocystis* sp. has not been fully determined.

The pathogenic potential of *Blastocystis* sp. remains controversial because many epidemiological and experimental animal studies have yielded different conclusions. Previous studies have shown that *Blastocystis* sp. infection causes gastrointestinal diseases, such as irritable bowel syndrome (IBS), ulcerative colitis, mysterious chronic urticaria, chronic spontaneous urticarial, and colorectal cancer [8–13]. A significant relationship between *Blastocystis* sp. and risk factors (age, sex, education, and residence) and clinical symptoms (stomach-ache and nausea) has been observed, while no significant relationship has been observed between bloating and diarrhea [14]. Moe et al. [15] found accumulated inflammatory cells, swollen lamina propria, and exfoliated mucosal cells in the intestine of mice infected with the parasite. Ajjampur et al. [16] found that similar symptoms occur after *Blastocystis* sp. infection in pigs. Puthia et al. [17] reported that *Blastocystis* ratti WR1 induced host cell apoptosis and altered intestinal epithelial barriers. Surprisingly, a study provided supportive data that *Blastocystis* sp. could exacerbate existing colorectal cancer via alteration in the host immune response and increased oxidative damage [9]. Given that *Blastocystis* sp. is a gut parasite, many researchers have theorized that the parasite may alter the intestinal microbiota and have attempted to explore the effect of the parasite on the host following the above idea. Yason et al. [18] reported that ST7 *Blastocystis* sp. infection reduces the number of beneficial *Bifidobacterium* and *Lactobacillus* in the intestine, possibly leading to an imbalance in the intestinal microecology. Although the above data suggest that *Blastocystis* sp. is a pathogenic microorganism, there are reports that *Blastocystis* sp. is a normal intestinal microorganism that does not affect the body. Castañeda et al. [19] found no significant difference in the composition of the intestinal flora between *Blastocystis*-positive and *Blastocystis*-negative children. A decrease in the relative abundance of *Bacteroides* and an increase in the relative abundance of *Faecalibacterium* was observed. However, they hypothesize that the presence of *Blastocystis* is unrelated to dysbiosis at the intestinal level and that it plays a role in the ecology of the intestinal microbiota through its interactions with other microbial components [19]. Stensvold et al. [20] postulate that *Blastocystis* sp. can promote host intestinal flora balance according to the α -diversity of intestinal microbiota in *Blastocystis* sp. carriers, which significantly increases, while β -diversity shows no significant difference. Moreover, Deng et al. [21] first confirmed that *Blastocystis* sp. ST4 has a good effect on intestinal symbiotic bacteria cultured in vitro, finding that ST4 can significantly inhibit the growth of *Bacteroides vulgatus* and

pathogenic *Bacillus*, speculating that ST4 may be a beneficial symbiotic subtype. In fact, *Blastocystis* sp. infection does change the normal structure of the intestinal microbiota, but whether this change is the main factor causing host discomfort is uncertain.

In recent years, apart from gut microbiota, host-expressed products and metabolites have gradually been recognized to play a key role in the health of the host. However, there is currently a lack of effective data to support the mechanism of interaction between *Blastocystis* sp. and its host. Therefore, in this study, transcriptomics, metabolomics, and intestinal microbiome analysis were combined to analyze the impact of *Blastocystis* sp. on hosts of different sex to understand the interactive mechanism of *Blastocystis* sp. and the host, determine its pathogenicity, and evaluate its public health significance.

2. Materials and Methods

2.1. Consent to Participate. Three-week-old BALB/c mice were purchased from Liaoning Changsheng Biotechnology Co., Ltd., and met ethical standards. Mice were bred and maintained in the animal facilities of Hebei Normal University providing freely accessible rodent chow and drinking water under controlled conditions. All mice were adapted for 1 week to the housing environment after purchase. When appropriate, the mice were anesthetized with an intraperitoneal injection of sodium pentobarbital (50 mg/kg), and the tested samples were quickly collected for subsequent experiments. No animals were harmed during the sampling process.

2.2. Parasite Culture and Preparation. *Blastocystis* sp. ST2 was identified and isolated from children's feces and preserved in the College of Life Science, Hebei Normal University [22]. The parasites were cultured anaerobically at 37°C in RPMI1640 medium containing 20% fetal bovine serum and ampicillin–streptomycin and subcultured every 2–3 days in the laboratory. After diluting the parasites, they were plated on a custom-made solid culture medium applying nutrients and ampicillin–streptomycin on the surface. Upon the growth of white colonies, they were collected and individually cultured in a medium and then obtained the parasites without impurities. *Blastocystis* sp. cysts were induced by trypsin in the medium before infecting mice.

2.3. Experimental Design. Twenty-four mice were divided into four groups: female control (FC) group, female test (FT) group, male control (MC) group, and male test (MT) group, with six mice in each group. The purified *Blastocystis* sp. were collected and diluted with PBS. The test group mice were orally inoculated with 1×10^5 parasites, whereas the control group was inoculated with an equal dose of PBS. On the 3rd and 5th days after inoculation, feces were collected from each mouse, and DNA was extracted for PCR detection to confirm successful infection. On the 5th day, whole blood, serum, and intestinal contents were collected for omics analysis.

2.4. Transcriptomic Analysis. Whole blood was collected from each mouse by eyeball bleeding, and total RNA was extracted

using TRIzol (Thermo Fisher Scientific, USA) according to the manufacturer's instructions. After the RNA quality control was passed, substandard cDNA libraries were obtained using AMPure XP beads using the screened mRNA. After qualified library checks, different libraries were pooled according to the amount of target on-machine data and sequenced using the Illumina HiSeq platform (Metware Biotechnology Inc.). The initial reads were obtained using Fastp, and the adapters, redundant sequences, and low-quality sequences were processed. The filtered reads were aligned with the mouse genome (*Mus musculus*. GRCm39.103) using the HISAT2. Transcripts were counted using featureCounts (1.6.1), and differentially expressed genes (DEGs) among different experimental groups were analyzed using DESeq2 (1.22.2) with reference values of $|\log_2FC| > 1$, $P < 0.01$, and false discovery rate (FDR) < 0.05 . The top 10 entries ($P < 0.05$) were selected for Kyoto encyclopedia of genes and genome (KEGG) pathway and GO functional enrichment analysis using the clusterProfiler package. Six differential genes, 1300017J02Rik, Bcl2l1, Atp5k, and Ube2s in females and Uqcr11 and Birc5 in males, were selected and verified by real-time quantitative PCR (RT-qPCR), and differential gene expression was considered significant when adjusted $P < 0.05$ by *t*-test using SPSS 20.0.

2.5. Metabolomic Analysis. Whole blood was collected from each mouse, and the serum was separated. The supernatants were extracted using a precooled extractant (20% acetonitrile methanol). The sample extracts were analyzed using an LC-ESI-MS/MS system (UPLC, Shim-pack UFLC SHIMADZU CBM A system, <https://www.shimadzu.com/>; MS, QTRAP[®] 6500+ System, <https://sciex.com/>). LIT and triple quadrupole (QQQ) scans were acquired on a triple quadrupole-linear ion trap mass spectrometer (QTRAP), QTRAP[®] 6500+ LC-MS/MS System, equipped with an ESI Turbo Ion-Spray interface, operating in positive and negative ion mode, and controlled by Analyst 1.6.3 (Sciex) (Metware Biotechnology Inc.). The abundance of metabolites was processed by MetaboDiff for missing values and normalized using the variance stabilizing normalization. Unsupervised PCA and supervised PLS-DA were then analyzed using ropls and mixOmics, and the variable importance point (VIP) value of each metabolite was calculated. Differential metabolites were screened according to two criteria: $VIP > 1$ and fold change > 2 ($P < 0.05$). The same significantly differential metabolite, heparin, was screened out from both females and males and verified by ELISA (Mouse Heparin Sodium (HS) ELISA Kit, Shanghai Enzyme-linked Biotechnology Co., Ltd.). R (version 4.2.2) analysis was performed on the data.

2.6. Microbiome Analysis. Each mouse was euthanized, and the intestinal contents were removed. The total DNA of each content was extracted using the hexadecyltrimethylammonium bromide (CTAB) method. After all DNA purity and concentration, libraries for 16S rRNA gene sequencing were prepared using Phusion[®] High-Fidelity PCR Master Mix with GC buffer (New England Biolabs Co., Ltd.) and V3/V4 specific primers (341F: 5'-CCTAYGGGRBGCASCAG-3', 806R: 5'-GGACTACNNGGGTATCTAAT-3') and TruSeq[®] DNA PCR-Free Sample Preparation Kit (Illumina, San Diego, USA).

The concentrations were quantitated by Qubit and Q-PCR, and the qualified libraries were sequenced using Nova-Seq6000 (Metware Biotechnology Inc.). The original raw tags were obtained by splicing the reads using FLASH (V1.2.7, <http://ccb.jhu.edu/software/FLASH/>) and then filtering using QIIME (V1.9.1, http://qiime.org/scripts/split_libraries_fastq.html). Effective tags were obtained after removing chimeric sequences by blasting the species annotation database (<https://github.com/torognes/vsearch/>). Operational taxonomic units (OTUs) were classified on the effective tags with 97% identity using Uparse software (Uparse v7.0.1001, <http://www.drive5.com/uparse/>). The representative sequence of each OTU was annotated using the RDP classifier (<http://rdp.cme.msu.edu/>) against the Silva 16S rRNA database using a confidence threshold of 99% to obtain taxonomic classifications at the phylum, class, order, family, and genus levels. Multiple sequence alignment was performed using QIIME (V1.9.1) to further explore the phylogenetic relationships between the different OTUs. QIIME used the Shannon index to describe alpha diversity. To determine beta diversity, UniFrac distance was calculated by QIIME and visualized by principal coordinate analysis using WGCNA, STATS, and GGPlot2 in R. Microbial functional enrichment and differential analysis were performed using PICRUST2 (Phylogenetic Investigation of Communities by Reconstruction of Unobserved States) and microbiomeMarker in R software. Microbiome abundance and diversity between different groups were calculated using the Wilcoxon rank-sum test (Wilcoxon) and plotted in R. The linear discriminant analysis effect size (LEfSe) method was used to compare the relative abundance of all bacterial taxa between groups [23]. This method emphasizes both statistical significance and biological relevance. An LDA score of > 4 and a Wilcoxon of < 0.05 were used as thresholds. In enrichment analysis, the visualization of microbiome functional enrichment results was completed in R, only showing entries with $P < 0.05$ and $FDR < 0.05$.

2.7. Joint Analysis of Multiomics Analysis. The normalized differential metabolites, genes, and microbes were subjected to Spearman's correlation coefficients. Representative products were obtained using mixOmics based on DIABLO (Data Integration Analysis for Biomarker Discovery using latent variable approaches for omics studies) modeling analysis. Strong correlations ($|\text{Spearman}| > 0.5$, $P\text{-value} < 0.05$) among products, metabolites, metabolites, microbes, and microbes were visualized using heat maps and Sankey diagrams. Metabolites serve as intermediaries linking the transcriptome to the microbiome. R analysis was performed on the data.

3. Results

3.1. Blastocystis sp. Causes the Differential Expression of Genes in Mice. Compared to the control group, the group of mice infected with *Blastocystis* sp. ST2 showed significant transcriptional differences in many genes related to inflammation, tumors, and neurological diseases. In female mice, there were 430 DEGs in the infection group (FT) compared with the control group (FC), 195 genes with upregulated

infection. The genes with downregulated expression were associated with oxidative phosphorylation and neurodegenerative diseases, including Parkinson's disease, Huntington's disease, and prion disease (Figure 1(c)). However, in males, 28 pathways were enriched, and genes with upregulated expression were mainly enriched in pathways such as neuroactive ligand–receptor interaction, IL-17 signaling pathway, and tuberculosis, and genes with downregulated expression had the same pathways as in females (Figure 1(d)).

GO analysis of post-ST2 *Blastocystis* sp. infection in mice demonstrated noteworthy changes in DEGs on diverse aspects, such as molecular function, biological processes, and cellular components. After conducting a comparative analysis, it was determined that most of the genes were annotated within the context of molecular function. In the female group, unigenes were annotated to 52 molecular functions. The genes with upregulated expression were mainly annotated as G protein-coupled receptor activity, peptide receptor activity, and G protein-coupled peptide receptor activity. The genes with downregulated expression were mainly annotated to proton transmembrane transporter activity, active transmembrane transporter activity, and primary active transmembrane transporter activity (Figure 2(a)). However, in males, unigenes were annotated to 77 molecular functions, the genes with upregulated expression were in transmembrane signaling receptor activity, immune receptor activity, and molecular transducer activity, and the genes with downregulated expression were annotated to oxidoreduction-driven active transmembrane transporter activity, electron transfer activity, and proton transmembrane transporter activity (Figure 2(b)). In terms of biological processes, these genes were annotated to 292 biological processes in females. The genes with upregulated expression were annotated to inflammatory response, cell motility, and cell migration, and the genes with downregulated expression were annotated to aerobic respiration and oxidative phosphorylation (Figure 2(c)). In males, the genes were annotated to 439 biological processes; the genes with upregulated expression were mainly involved in myeloid leukocyte activation, innate immune response, and inflammatory response, and the genes with downregulated expression were mainly involved in proton motive force-driven mitochondrial ATP synthesis and mitochondrial respiratory chain complex assembly (Figure 2(d)). In terms of cellular components, in the females, the genes were in 46 cellular components, the genes with upregulated expression were mainly in the cell surface, cell periphery, and plasma membrane, and the genes with downregulated expression were mainly in the mitochondrial protein-containing complex and inner mitochondrial membrane protein complex (Figure 2(e)). In males, the genes were in 71 cellular components, and the genes with upregulated expression were mainly in the cornified envelope, trans-Golgi network, and Golgi apparatus subcompartment, while the genes with downregulated expression were mainly in the catalytic complex, inner mitochondrial membrane protein complex, and mitochondrial protein-containing complex (Figure 2(f)). From the above data, six genes with downregulated expression were screened: 1300017J02Rik, *Bcl2l1*, *Atp5k*, and *Ube2s* in females and *Uqcr11* and *Birc5* in males ($P < 0.05$)

and verified by RT-qPCR. These results were consistent with the transcriptomic results (Figure 2(g)), showing the reliability of the transcriptomic data.

3.2. *Blastocystis* sp. Infection Causes Metabolic abnormalities in Mice. To analyze the sample data space by principal components analysis, we assumed the reliability of the data and showed significant changes in metabolites between groups. The result of the volcano plot analysis displayed 82 differential metabolites in female mice and 118 differential metabolites in male mice, respectively. Twenty-seven metabolites with upregulated expression, such as MEDN1135 (heparin), MW0124717 (L-stercobilinogen), and MW0062279 (prostaglandin K2), and 55 metabolites with downregulated expression, such as MEDN1287 (LPE(0:0/16:1)), MEDN1400 (4-methoxy salicylic acid), and MW0129705 (1,7-Bis(4-hydroxyphenyl)-4-hepten-3-one), were screened in females (Figure 3(a)). Moreover, 24 metabolites with upregulated expression, such as MEDN1139 (DL-2-hydroxystearic acid), MEDN1135 (heparin), and MW0123384 (clerodin), and 94 metabolites with downregulated expression, such as MEDN0244 (orotic acid), MEDN0287 (3,5-dimethoxy-4-hydroxycinnamic acid), MEDN1245 (2-benzylmalate), and MW0151330 (Ile-Arg-Ile-Ile-Val) were screened in males (Figure 3(b)). The above differential metabolites were matched to the KEGG database to identify the pathways in which the metabolites might participate. The results of enrichment analysis showed that differential metabolites in the females were mainly enriched in pathways such as pyrimidine metabolism, synthesis and degradation of ketone bodies, and linoleic acid metabolism (Figure 3(c)) and that in males were mainly involved in phenylalanine metabolism, linoleic acid metabolism, synthesis, and degradation of ketone bodies (Figure 3(d)). Surprisingly, the level of heparin in all mice infected by *Blastocystis* sp. increased significantly and then was redetected by the enzyme-linked immunosorbent assay (ELISA). The standard curve was $y = 0.0029x + 0.722$ and $R^2 = 0.9927$ (Figure 3(e)), indicating a good fit for the experiment. Analysis of heparin concentration showed that their levels were significantly higher in the test groups than in the control groups. This was consistent with the results of metabolomics and showed the reliability of omics (Figure 3(f)).

3.3. Intestinal Microecology Was Changed by *Blastocystis* sp. in Mice. The alteration of the intestinal flora in each group was observed based on high-throughput sequencing. Compared with the control group, the species evenness of Lachnospiraceae decreased, but that of Muribaculaceae and Bacteroidaceae increased in *Blastocystis*-infected female mice, and the same trend was observed in males (Figure 4(a)). LDA effect size (LEfSe) analysis showed a significant difference in the abundance of Rhodobacteraceae in females infected with *Blastocystis* sp. At the species level, the xylanophilum group-uncultured bacteria, Ruminococcaceae_uncultured, and *Helicobacter typhlonius* showed significant differences in abundance. In males, there were significant differences in the abundance of Muribaculaceae, Bacteroidaceae, Prevotellaceae, Flavobacteriaceae, and Tannerellaceae. At the species

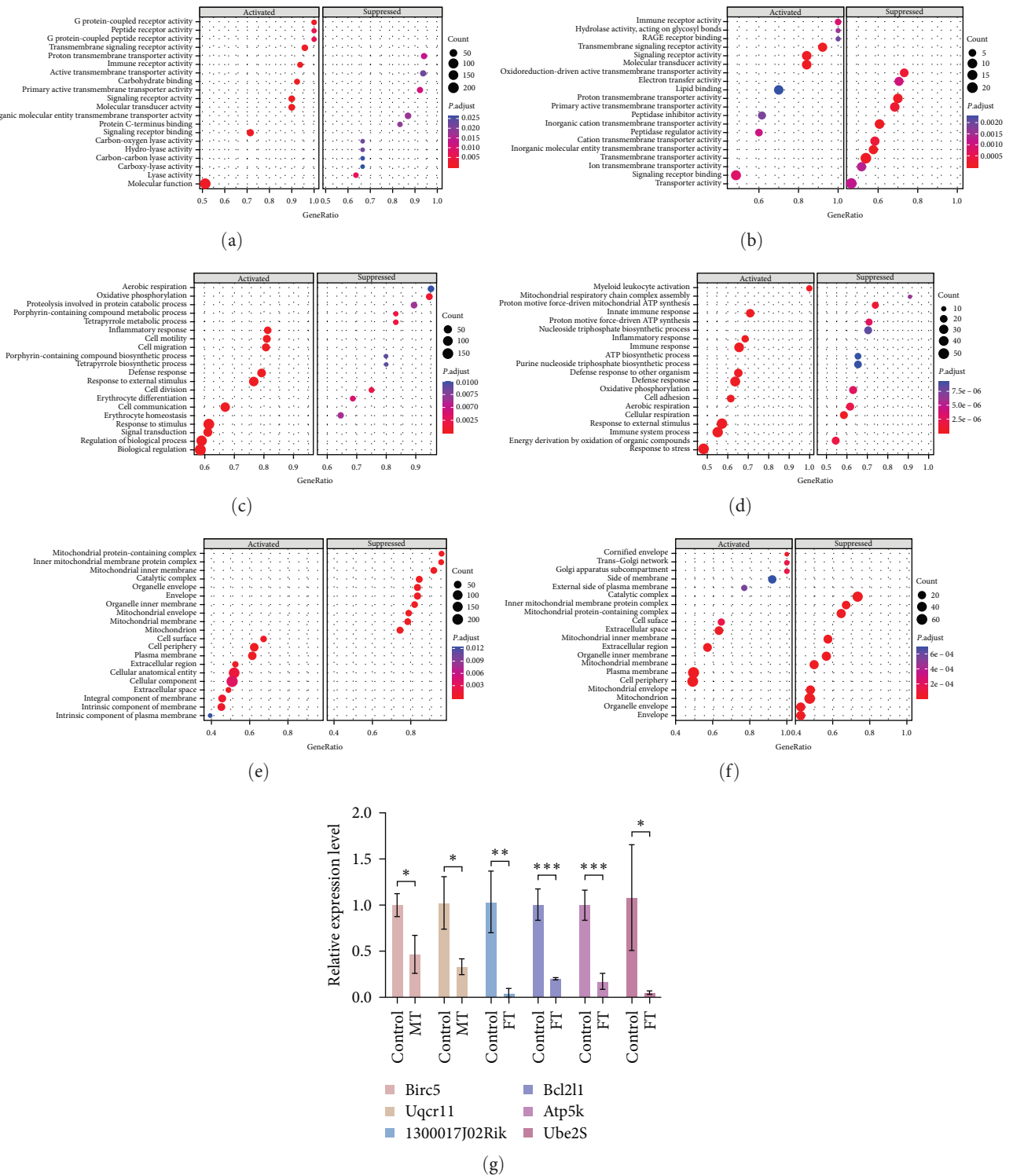


FIGURE 2: Molecular function GO enrichment scatter plots. (a) Molecular function GO enrichment scatter plots for the FC and FT groups. (b) Molecular function GO enrichment scatter plots for the MC and MT groups. (c) Biological process GO enrichment scatter plots for the FC and FT groups. (d) Biological process GO enrichment scatter plots for the MC and MT groups. (e) Cellular component GO enrichment scatter plots for the FC and FT groups. (f) Cellular component GO enrichment scatter plots for the MC and MT groups. (g) Verification results of qRT-PCR. GAPDH was the internal parameter, the data (multiple changes) were log₂, expressed as mean ± SD, and the normal control group (log₂ = 1) (n = 5) was used as the control. *P < 0.05, **P < 0.01, ***P < 0.001.

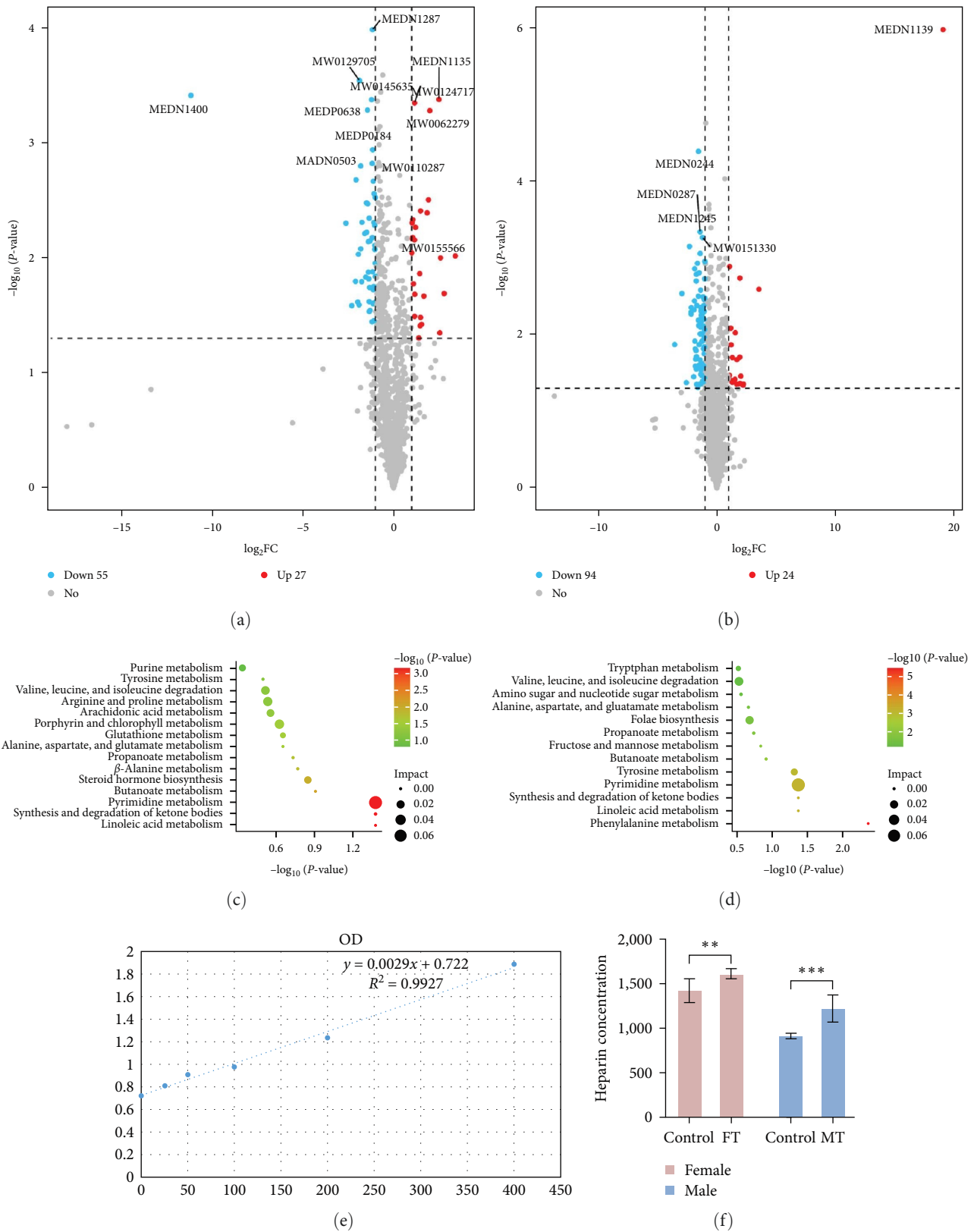
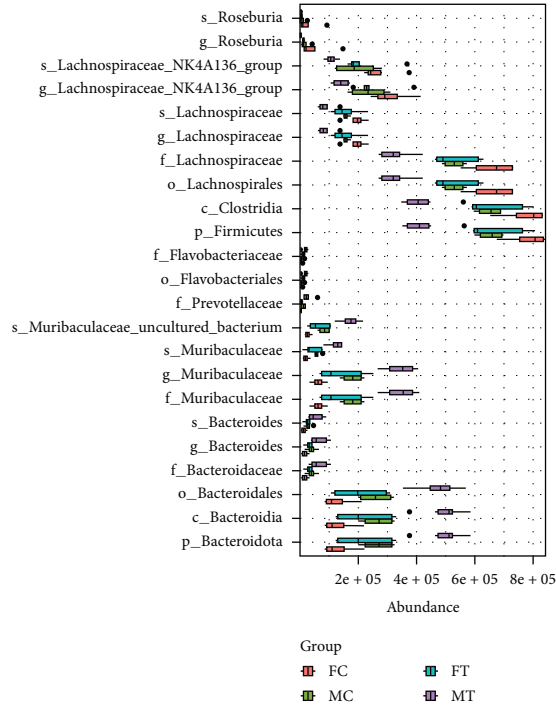
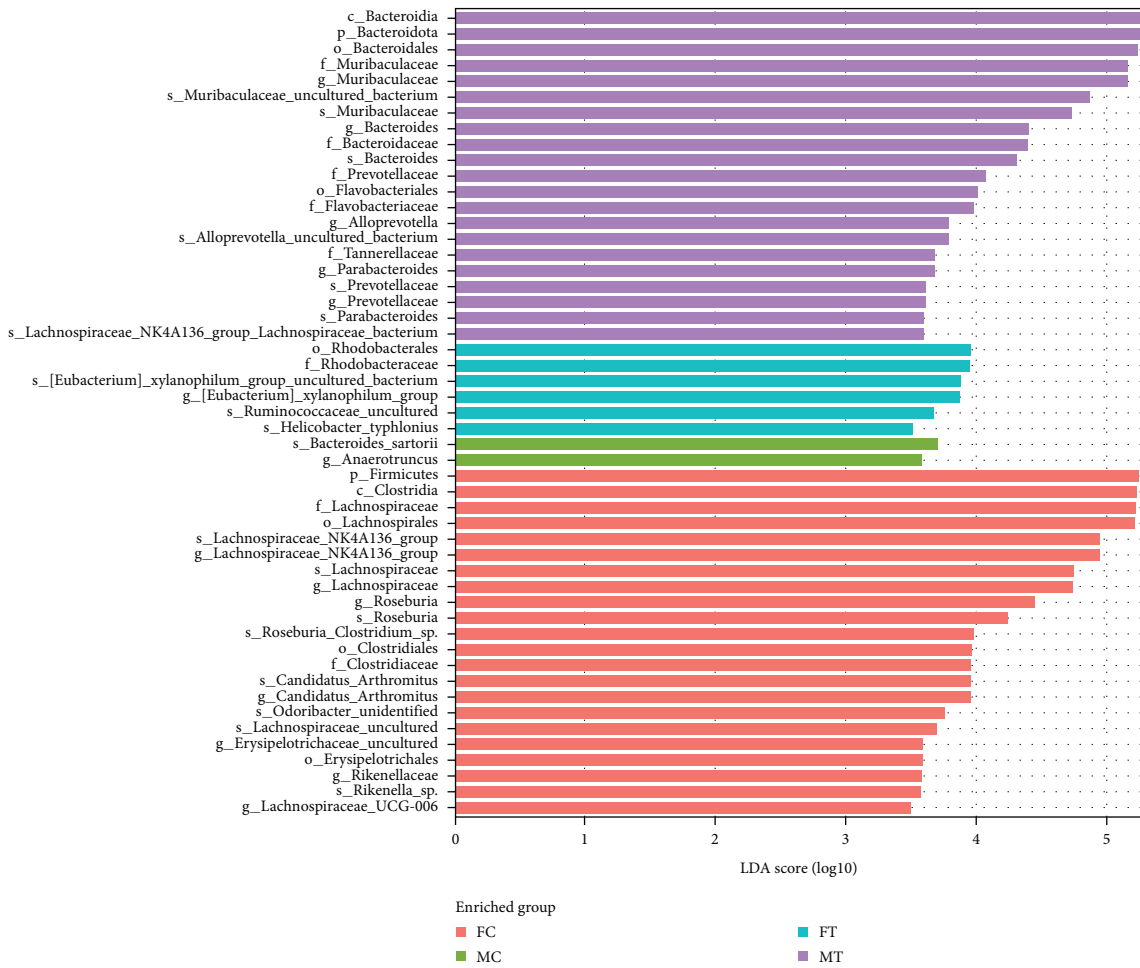


FIGURE 3: *Blastocystis* sp. infection causes metabolic abnormalities in mice. (a) Differential metabolite volcano plot of the female control group (FC) and female experimental group (FT). (b) Differential metabolite volcano plot of the male control group (MC) and the male experimental group (MT). (c) KEGG enrichment scatter plot of the female control group (FC) and female experimental group (FT). (d) KEGG enrichment scatter plot of the male control (MC) and male experimental (MT) groups. (e) Standard curve. (f) Verified results of the heparin ELISA test ($n = 5$), ** $P < 0.01$, *** $P < 0.001$.



(a)



(b)

FIGURE 4: Continued.

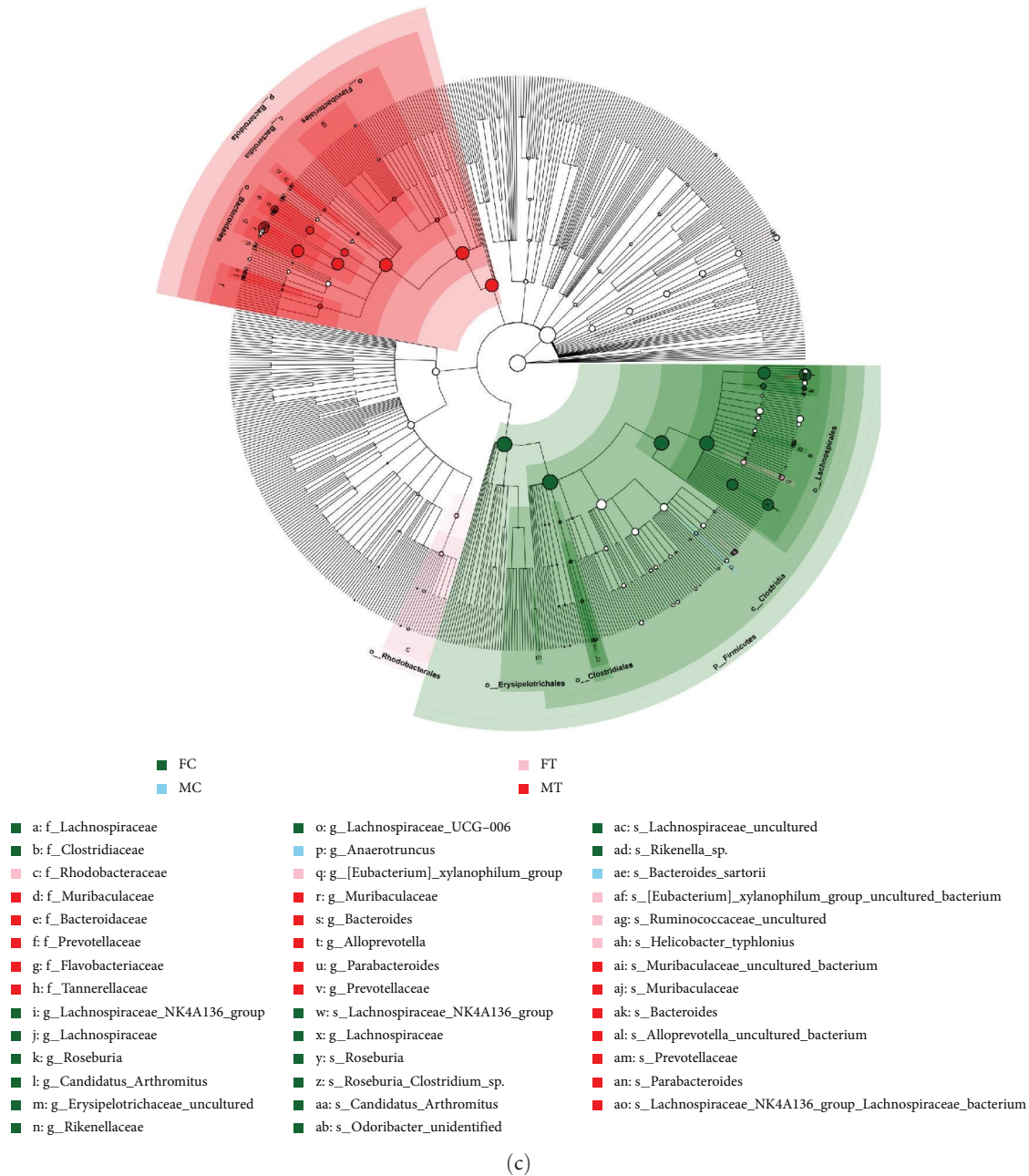


FIGURE 4: Changes in the intestinal microecology of *Blastocystis* sp. in mice: (a) gut microbiota abundance, (b) histogram of the LDA value distribution, and (c) gut microbiota evolutionary analysis.

level, Muribaculaceae uncultured bacteria, Muribaculaceae, Bacteroides, Alloprevotella uncultured_bacteria, Prevotellaceae, Parabacteroides, and Lachnospiraceae NK4A136 groups showed significant differences in abundance (Figures 4(b) and 4(c)).

3.4. Joint Analysis of Transcriptomics and Metabolomics. Spearman correlation coefficients were obtained by combining the transcriptomic and metabolomic methods. Heat maps were used to determine the correlation between DEGs and metabolites. In females, 329 genes correlated with 82

differential metabolites in the range of $0.01 < P < 0.05$, 253 genes correlated with 76 metabolites in the range of $0.001 < P < 0.01$, and 205 genes correlated with 50 metabolites in the range of $P < 0.001$ (Figure 5). Similarly, in males, 366 genes correlated with 118 differential metabolites in the range of $0.01 < P < 0.05$, 246 genes correlated with 114 metabolites in the range of $0.001 < P < 0.01$, and 145 genes correlated with 74 metabolites in the range of $P < 0.001$ (Figure 6). The association products were diverse; however, the family factors of *Ifitm* and *Wfdc* remained highlighted. In all mice, many metabolites were positively and negatively correlated

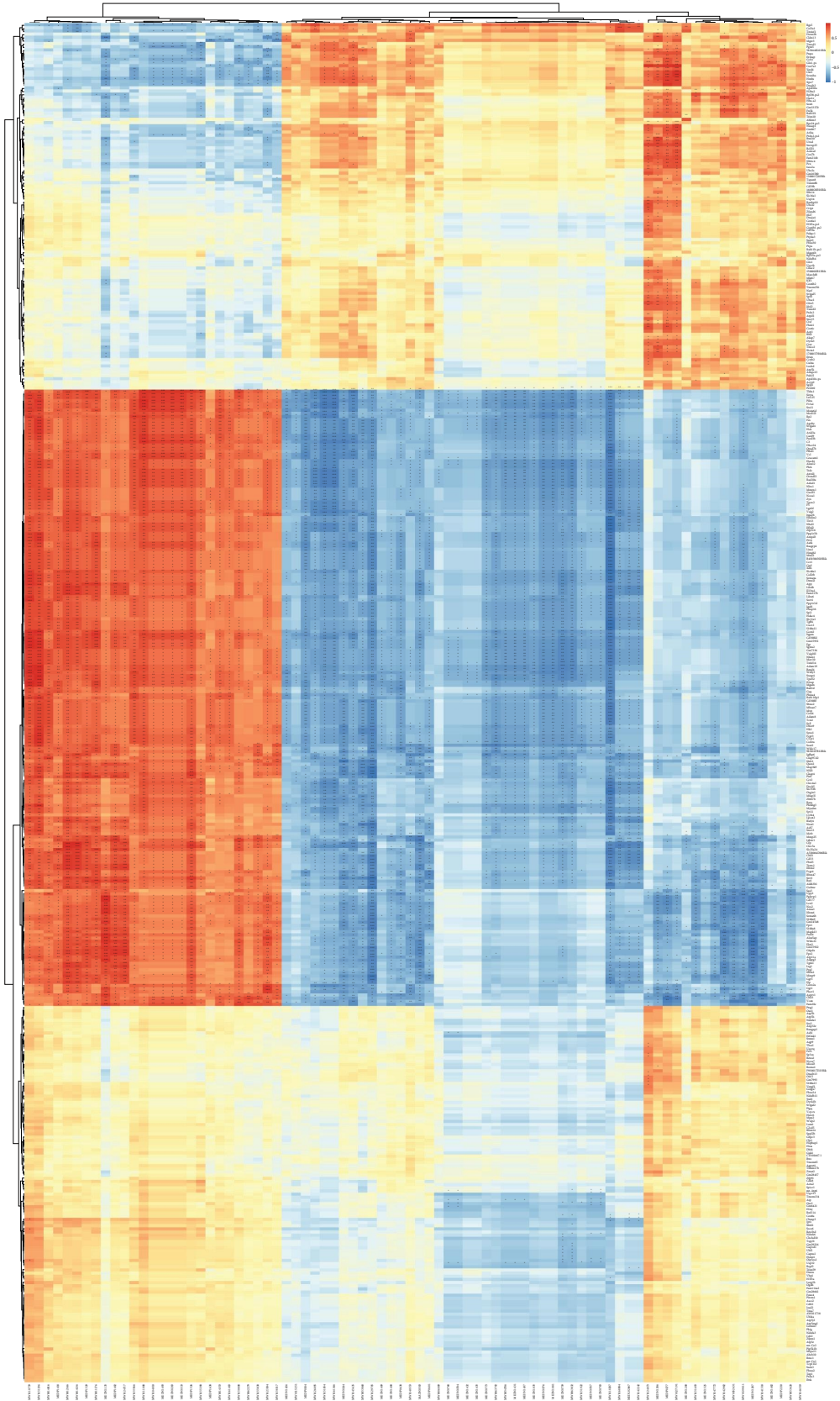


FIGURE 5: Heat map of combined transcriptome and metabolome analysis of female mice infected with *Blastocystis* sp. ST2. $+0.01 < P < 0.05$, $++0.001 < P < 0.01$, $+++P < 0.001$.

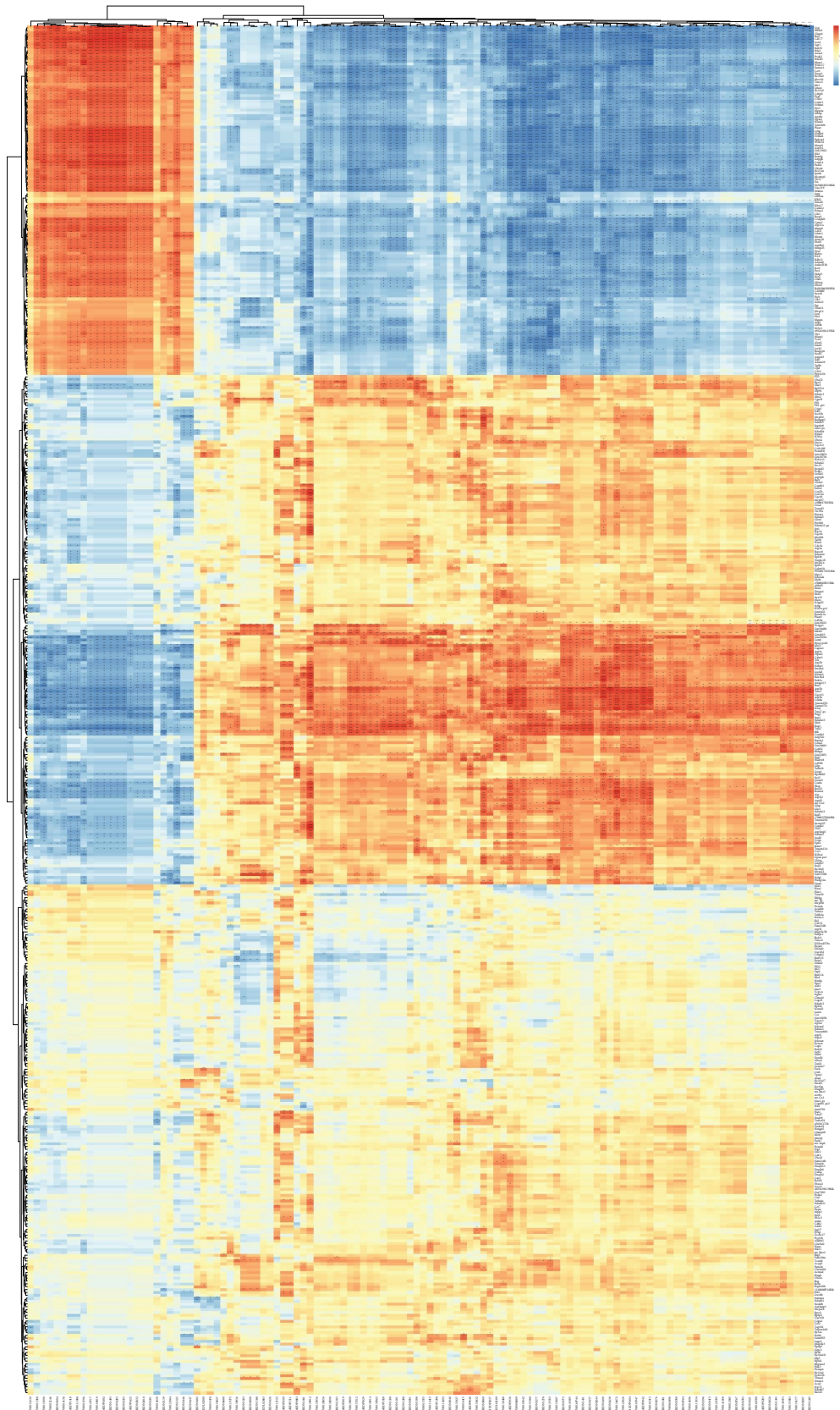


FIGURE 6: Heat map of combined transcriptome and metabolome analysis of male mice infected with *Blastocystis* sp. ST2. $+0.01 < P < 0.05$, $++0.001 < P < 0.01$, $+++P < 0.001$.

with the two factors; most significantly, *Wfdc* and *Ifitm* were positively correlated with heparin and negatively correlated with LPEs. Interestingly, there were more highly significant association products in male mice than in female mice.

3.5. Joint Analysis of Transcriptomics and Microbiome. At the class level, it was found that microbes significantly correlated with DEGs were mainly concentrated in Clostridia, Bacteroidia, and Alphaproteobacteria in the females by associating the transcriptomics with the microbiome. Clostridia was significantly negatively correlated with *Plxna4* gene ($P < 0.001$) and significantly positively correlated with *Vcan*, *Chil3*, and *Fam20c* genes ($P < 0.001$). Bacteroidia were significantly negatively correlated with *Fam20c* and *Vcan* genes ($P < 0.001$) and significantly positively correlated with the *Hmbs* gene ($P < 0.001$) (Figure 7). Similarly, in males, microbes that were significantly correlated with DEGs were mainly concentrated in Clostridia and Bacteroidia. Among them, Clostridia was significantly negatively correlated with the *Slc16a3* gene ($P < 0.001$) and significantly positively correlated with *Pla2g12a* and *Gm4013* genes ($P < 0.001$). Bacteroidia were significantly positively correlated with *Dusp1*, *Slc16a3*, and *Arg2* genes ($P < 0.001$) and significantly negatively correlated with *Elob*, *Atp5h*, and *Mki67* genes ($P < 0.001$) (Figure 8).

3.6. Join Analysis of Metabolomics and Microbiome. Through a joint analysis of metabolomics and microbiome data, we aimed to understand host systematic changes in gut microbes and metabolites after *Blastocystis* sp. ST2 infection. At the class level, it was found that microbes significantly correlated with differentially expressed metabolites were mainly concentrated in Clostridia, Alphaproteobacteria, and Bacteroidia in females. Among them, Clostridia was significantly positively correlated with MW0062279 (prostaglandin K2) ($P < 0.001$), Alphaproteobacteria and Bacteroidia were significantly positively correlated with MW0014816 (5-octynoic acid, 8-hydroxy-8-[2-(pentyloxy)phenyl]-, methyl ester) ($P < 0.001$), Clostridia was significantly negatively correlated with MW0139011 (Mulberrofuran E), MW0127191 (1-isothiocyanatopentane) and MEDP0277 (methyl indole-3-acetate) ($P < 0.001$), and Bacteroidia was significantly negatively correlated with MEDN0376 (9,10-DiHOME) and MEDN1081 (12,13-DiHOME) ($P < 0.001$), respectively (Figure 9). However, in males, microbes that were significantly correlated with differentially expressed metabolites were mainly concentrated in Clostridia and Bacteroidia. Among them, Clostridia was significantly negatively correlated with MEDN1139 (DL-2-hydroxystearic acid), MW0011596 ((R)-8-Acetoxyarvotanacetone), MW0123384 (clerodin), and MEDN1135 (heparin) ($P < 0.001$), and significantly positively correlated with MW0139362 (pinocembrin), MW0114292 (diphenol glucuronide), MEDN0121 (enterodiol), MEDN0244 (orotic acid), MW0138514 (isoquercitrin; quercetin 3-O-glucoside), MW0157312 (swertianin; 1,2,8-trihydroxy-6-methoxyxanthone), MEDN1426 (9(S),12(S),13(S)-TriHOME), and MEDL02603 (3',4',7-trihydroxyflavone) ($P < 0.001$). Bacteroidia was

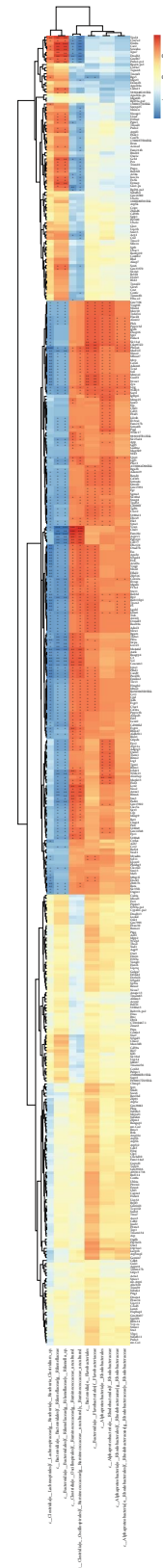


FIGURE 7: Heat map of combined transcriptome and microbiome analysis of female mice infected with *Blastocystis* sp. ST2. +0.01 $< P < 0.05$, ++0.001 $< P < 0.01$, +++ $P < 0.001$.

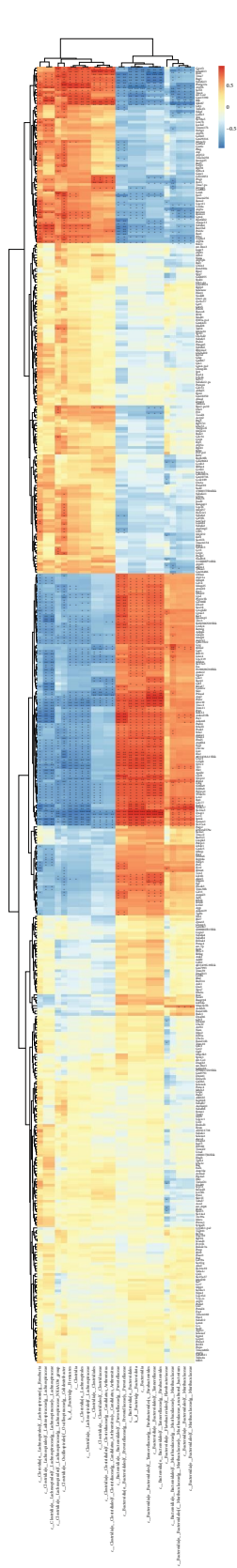


FIGURE 8: Heat map of combined transcriptome and microbiome analysis of male mice infected with *Blastocystis* sp. ST2. +0.01 < P < 0.05, ++0.001 < P < 0.01, +++P < 0.001.

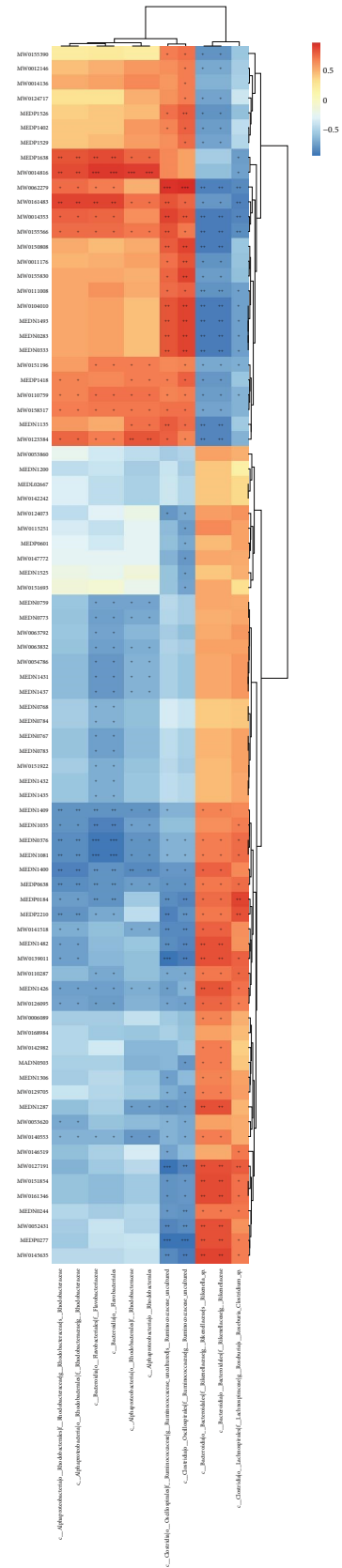


FIGURE 9: Heat map of combined analysis of metabolome and microbiome of female mice infected with *Blastocystis* sp. ST2. +0.01 < P < 0.05, ++0.001 < P < 0.01, +++P < 0.001.

significantly positively correlated with MW0123384 (clerodin) ($P < 0.001$) and negatively correlated with MW0123226 (carbofuran), MEDN0287 (3,5-dimethoxy-4-hydroxycinnamic acid), MEDN1245 (2-benzylmalate), MEDP1404 (carnitine C14:2-OH), MW0107947 (L-pyridosine), MEDP1298 (pregnanetriol), MW0114292 (diphenol glucuronide), MEDN0121 (enterodiol), MEDP0203 (trans-Cinnamaldehyde), MEDN1426 (9(S), 12(S),13(S)-TriHOME), MEDN0244 (orotic acid), MW0138514 (isoquercitrin; quercetin 3-O-glucoside), MW0157312 (swertianin; 1,2,8-trihydroxy-6-methoxyxanthone), MEDL02603 (3',4',7-trihydroxyflavone), and MEDN1630 (ferulic acid) ($P < 0.001$) (Figure 10).

3.7. Joint Analysis of Transcriptomics, Metabolomics, and Microbiome. Through joint analysis of the transcriptome, metabolome, and microbiome, correlations among the three omics were exhibited (Figure 11). In females, the associated microbes were mainly concentrated in the Clostridia, Bacteroidia, and Alphaproteobacteria classes, which were associated with 301 differential genes and 128 differential metabolites ($P < 0.05$) (Supplementary 1). However, the associated microbes were mainly concentrated in the Clostridia and Bacteroidia classes, associated with 307 differential genes and 158 differential metabolites in males ($P < 0.05$) (Supplementary 2).

4. Discussion

Blastocystis sp. is a single-celled anaerobic eukaryotic parasite that is distributed worldwide. There are conflicting views on whether it causes disease in humans, although it has recently been linked to IBS [24]. The genetic diversity of this organism might contribute to the uncertainty regarding its role in the disease, particularly if not all subtypes have the same effect on the host. At present, there are no reports on differences in host transcriptomics and metabolomics caused by *Blastocystis* sp. Therefore, joint transcriptomic, metabolomic, and intestinal microbiome analyses were used to study the impact of *Blastocystis* sp. ST2 on the host in our study subject. Our results showed that significant changes occurred in transcription and metabolite levels and gut microbiota in mice infected with *Blastocystis* sp. ST2. However, we primarily focused on many factors in all omics associated with tissue inflammation. Previous studies have shown that *Blastocystis* sp. can cause changes in the blood, with a significant decrease in white blood cell count, hemoglobin, and hematocrit levels [25, 26]. Through the construction of a mouse model, it was confirmed that *Blastocystis* sp. caused damage to the intestinal mucosa, and pathological observation showed that the ultrastructure of the intestinal mucosal cells was significantly changed, including partial shedding of intestinal microvilli, damage to mucosal epithelial cells, local edema of mitochondria, and disordered arrangement of ridges [15, 16, 18]. The above phenomena suggest the potential harm, and we speculate that the above intestinal injuries are associated with the inflammation caused by *Blastocystis* sp. Significantly DEGs in the transcriptome are mainly related to the inflammatory response, cancer

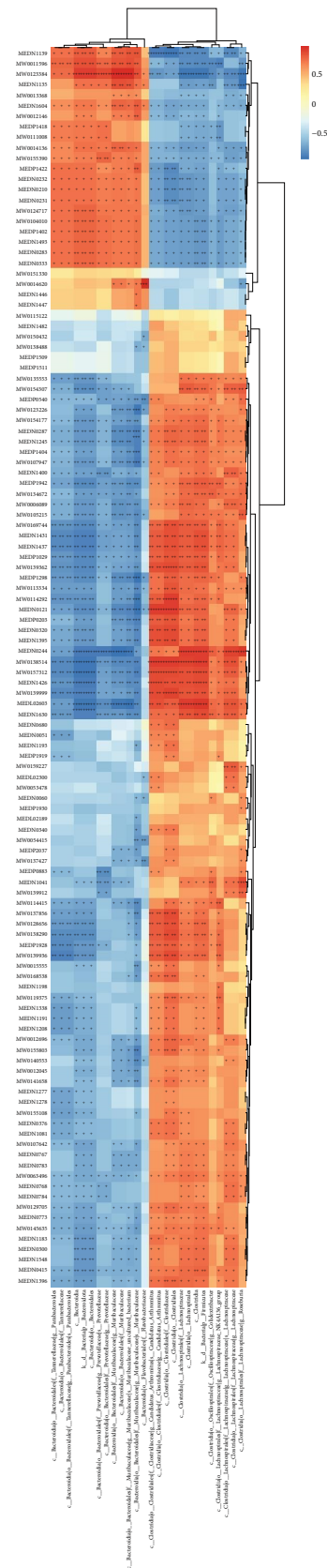


FIGURE 10: Heat map of the combined analysis of metabolome and microbiome of male mice infected with *Blastocystis* sp. ST2. +0.01 $< P < 0.05$, ++0.001 $< P < 0.01$, +++ $P < 0.001$.

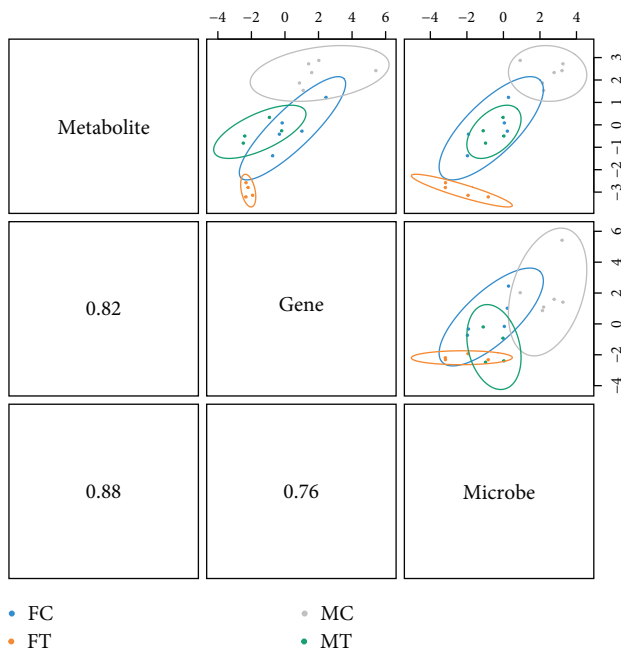


FIGURE 11: Transcriptome, metabolome, and microbiome combined analysis.

tumor occurrence, immune function, and neurological diseases. Interestingly, the transcription level of *Ifitm1* was significantly upregulated in all mice. Many studies have shown that *Ifitm1* is a marker for colorectal cancer and participates in the tumorigenesis process, and from previous studies, the overexpression of this gene could increase the probability of tumor occurrence [27]. Similarly, Kelemen et al. [28] also found that *Ifitm1*, as a negative regulator of cell proliferation, plays a key role in tumor formation according to the overexpression of the gene in tumor epithelial cells of human squamous cell carcinoma and adenocarcinoma in NSCLC patients. Coincidentally, *Blastocystis* sp. usually colonizes and damages the gut; therefore, we suspected that the parasite induces tumor formation. Moreover, parasite infection causes abnormal expression of host genes linked to the tumor. In female mice, the transcription level of *Xpo7* was significantly downregulated, and the gene is a new type of tumor suppressor that controls aging and tumor occurrence by regulating the expression of P21^{CIP1} in a previous study [29]. In male mice, upregulation in the expression of *Adam8* and downregulation in the expression of *Tuba1b* were observed. *Adam8* has been considered an important participant in invasive malignant tumors, including breast cancer, pancreatic cancer, and brain cancer, and *Tuba1b*, as a key regulator of osteosarcoma and is related to the lifetime of colon adenocarcinoma [30–32]. GO analysis revealed that after the host was infected with *Blastocystis* sp. ST2, inflammatory and immune responses occurred, which was reflected by the IL-17 signaling pathway in KEGG analysis. IL-17 is a cytokine that drives autoimmune and inflammatory diseases and promotes tumor progression in pathological environments. In addition, the *Wfdc* family members in all mice were matters of concern because of their functions in sperm

maturation, inflammation, and innate immunity, especially *Wfdc17* and *Wfdc21* [33–37]. Interestingly, many differential factors, such as upregulated and downregulated expression of *RARα* and *Hmbs* genes, respectively, in females and downregulated expression of *Cox7b* in male mice, are similar to the host symptoms, IBS. *RARα* plays a crucial role in the selective activation of pro-inflammatory and anti-inflammatory signals, the absence of *Hmbs* can cause acute intermittent porphyria, leading to abdominal pain, neuropsychiatric disorders, and neuropathy, and *Cox7b* plays an important role in normal development of the central nervous system in vertebrates [38, 39]. Of course, it is one-sided to affirm *Blastocystis* sp. as a stimulating factor for immune diseases and tumor occurrence just by the aberrant transcripts of many genes. However, that has an important reference sense for further exploring the interaction mechanism between *Blastocystis* sp. and the host.

Changes in host metabolites caused by pathogens may cause physical illness. Many metabolites have been screened by metabolomics analysis in mice of different sex infected with *Blastocystis* sp. ST2. However, we screened and focused on several differential metabolites shared by all mice, including heparin, 4-methoxy salicylic acid, and clerodin. In a previous study, heparin had anti-inflammatory and antitumor effects [40–42], which is consistent with the effects shown by differential genes, supporting the speculation that *Blastocystis* sp. ST2 may cause pathological changes such as an inflammatory response in the host. Merida-de-Barros et al. [43] found that heparin was produced by resident white blood cells, involved in the inflammatory response, such as mast cells, and could be present at lesion sites and bind to specific receptors to release activity. Lantero et al. [44] considered heparin exhibits antimalarial activity. Thus, heparin may have an inhibitory effect on *Blastocystis* sp. and may be a protective mechanism by which the body appears to resist *Blastocystis* sp. damage. In addition to heparin, many metabolites, such as 10-hydroxydecanoic acid and 4-methylsalicylic acid, have been proven to be associated with tissue inflammation [45]. The causes of inflammation are diverse and complex, and *Blastocystis* sp. is one of the important factors based on the combined analysis of transcriptomic and metabolomic data.

Another aspect of parasite pathogenicity is expressed in the intestinal flora. However, at present, the conclusions of the study of *Blastocystis*–host interactions through the intestinal microbiome are divided. Stensvold et al. [20] and Castañeda et al. [19] hypothesized that *Blastocystis* sp. is a normal microbe in the host intestine and plays an important role in regulating intestinal flora ecology. Deng et al. [21] demonstrated that *Blastocystis* sp. ST4 could inhibit the growth of pathogenic *B. vulgatus* and suggested ST4 was a beneficial commensal. However, Nagel et al. [46] analyzed the intestinal flora of patients with IBS infected with *Blastocystis* sp. and found significant differences in the fecal microbiota between patients with diarrhea-predominant IBS and healthy controls; however, the carriage of *Blastocystis* sp. did not significantly alter the fecal microbiota. Deng et al. [47] confirmed that *Blastocystis* sp. ST2 coinfects with *Clostridium difficile*

can cause life-threatening diarrhea and colitis. It is speculated that *Blastocystis* sp. ST2 may cause diarrhea in the host, but the pathogenicity of the parasite is different owing to its heterogeneity among subtypes. According to the established network relationships of the three omics, transcriptomic, metabolomic, and microbiome, Clostridia are an important microbial group that is directly or indirectly connected with transcripts and metabolites in mice infected with *Blastocystis* sp. ST2. This further indicates that *Blastocystis* sp. ST2 may damage the intestinal microecological imbalance, leading to diarrhea or pathogenicity. In this study, after *Blastocystis* sp. ST2 infection in mice, significant changes were observed in the intestinal flora, among which differences in Firmicutes and Bacteroidota were the most significant. In a previous study, the ratio of Firmicutes/Bacteroidetes (F/B ratio) was found to be a factor related to complications such as diabetes, obesity, or inflammatory bowel disease [48]. The results of this study showed that the F/B ratio decreased in mice infected with *Blastocystis* sp. ST2. This was consistent with Yañez et al.'s [48] study on *Blastocystis* sp. ST1 and ST7 and Maritat's study [49] on *Blastocystis* sp. ST4 causing changes in host intestinal microbes. Furthermore, it is speculated that IBS and weight loss may be related to the parasite. In addition, this study showed that Rhodobacterales were more abundant in the intestines in female mice infected with *Blastocystis* sp., consistent with the results of Kodio's study [50] on the changes in intestinal floras in children infected with *Blastocystis* sp.. Muribaculaceae and Prevotellaceae were two important groups of microbes in male mice infected with the parasite, consistent with the results from Kim's and Audebert's research [51, 52]. The content of other microbes, such as Lachnospiraceae, also changed with the action of *Blastocystis* sp. ST2 in mice, but their roles still require further exploration and verification. There were significant differences in gut flora between male and female mice after infection with *Blastocystis* sp. ST2, which may be related to host immunity and physiological characteristics; however, further research is required to determine whether sex effects modified the association.

In the joint analysis of transcriptomics and metabolomics, we established data relationships among different levels of molecules, combined functional analysis and metabolic pathway enrichment, and performed a correlation analysis between metabolites and microbes to achieve a comprehensive understanding of the general trend and direction of biological changes. According to the established network relationships of transcriptomic, metabolomic, and microbiome analyses, it is possible that there were some positive or negative interaction effects among the transcripts, metabolites, and microbes. However, it is very complicated in an organism and requires a lot of research data to determine how it works. The mechanism through which *Blastocystis* sp. impacts the host was studied initially, and the research data provided basis for our future research; however, complete understanding of the underlying mechanism remains elusive. We focused on inflammation, but the causes of inflammation are diverse and complex. Therefore, further in-depth research

is required to determine the roles of each inflammatory factor. Additionally, the data showed subtle differences, and many studies are needed to determine whether the relationship between *Blastocystis* sp. and the host is affected by hormones.

5. Conclusion

Based on the analysis of transcriptomics, metabolomics, and microbiome, it is concluded that *Blastocystis* sp. ST2 infection causes significant changes in the transcript and metabolic profile of the host, as well as intestinal microecological imbalance, and it is confirmed that *Blastocystis* sp. ST2 infection is harmful to the host. These results provide insight into the mechanism of *Blastocystis*–host interactions.

Data Availability

The data supporting the findings of this study are available from the corresponding author upon reasonable request.

Ethical Approval

This study complied with the guidelines of the Regulations for the Administration of Affairs Concerning Experimental Animals and was approved by the Biomedical Ethical Committee of Hebei Normal University, Hebei, China (ID: 2022LLSC024).

Conflicts of Interest

The authors declare that they have no conflicts of interest.

Authors' Contributions

All authors participated in the collection of samples and performed the laboratory tests and analysis. Cao Mengjuan and Zhang Shaojun analyzed the results. Ma Lei and Nan Huizhu designed the study and wrote the manuscript. Cao Mengjuan, Zhang Shaojun, and Nan Huizhu are co-first authors; order determined by relative overall contributions.

Acknowledgments

This work was supported by the Hebei Natural Science Foundation (no. H202105002), the S&T Program of Hebei Province, China (no. 22326703D), the S&T Program of Shijiazhuang, Hebei (225500395A), and China Postdoctoral Science Foundation (no. 2019M651061). Funding was provided by Hebei Provincial Department of Science and Technology, Shijiazhuang Municipal Bureau of Science and Technology, and China Postdoctoral Science Foundation.

Supplementary Materials

Supplementary 1. Sankey map of the combined transcriptome, metabolome, and microbiome analysis of female mice infected with *Blastocystis* sp. ST2.

Supplementary 2. Sankey map of transcriptome, metabolome, and microbiome of male mice infected with *Blastocystis* sp. ST2.

References

- [1] C. R. Stensvold, G. K. Suresh, K. S. W. Tan et al., “Terminology for *Blastocystis* subtypes—a consensus,” *Trends in Parasitology*, vol. 23, no. 3, pp. 93–96, 2007.
- [2] C. Noël, F. Dufernez, D. Gerbod et al., “Molecular phylogenies of *Blastocystis* isolates from different hosts: implications for genetic diversity, identification of species, and zoonosis,” *Journal of Clinical Microbiology*, vol. 43, no. 1, pp. 348–355, 2005.
- [3] J. Forsell, M. Granlund, C. R. Stensvold, G. C. Clark, and B. Evengård, “Subtype analysis of *Blastocystis* isolates in Swedish patients,” *European Journal of Clinical Microbiology & Infectious Diseases*, vol. 31, no. 7, pp. 1689–1696, 2012.
- [4] K. S. W. Tan, “New insights on classification, identification, and clinical relevance of *Blastocystis* spp.,” *Clinical Microbiology Reviews*, vol. 21, no. 4, pp. 639–665, 2008.
- [5] Cotruvo and A. Joseph, “WHO guidelines for drinking water quality: first addendum to the fourth edition,” *American Water Works Association*, vol. 109, no. 7, pp. 44–51, 2017.
- [6] M. A. Alfellani, D. Taner-Mulla, A. S. Jacob et al., “Genetic diversity of *Blastocystis* in livestock and zoo animals,” *Protist*, vol. 164, no. 4, pp. 497–509, 2013.
- [7] M. Santin, A. Figueiredo, A. Molokin et al., “Division of *Blastocystis* ST10 into three new subtypes: ST42-ST44,” *Journal of Eukaryotic Microbiology*, vol. 71, no. 1, Article ID e12998, 2024.
- [8] M. Kök, Y. Çekin, A. H. Çekin, S. Uyar, F. Harmandar, and Y. Şahintürk, “The role of *Blastocystis hominis* in the activation of ulcerative colitis,” *Turkish Journal of Gastroenterology*, vol. 30, pp. 40–46, 2019.
- [9] V. Kumarasamy, W. M. Atroosh, D. Anbazhagan, M. M. I. Abdalla, and M. Azzani, “Association of *Blastocystis hominis* with colorectal cancer: a systematic review of *in vitro* and *in vivo* evidences,” *World Journal of Gastrointestinal Oncology*, vol. 14, no. 3, pp. 734–745, 2022.
- [10] M. Lepczyńska, W.-C. Chen, and E. Dzika, “Mysterious chronic urticaria caused by *Blastocystis* spp.?” *International Journal of Dermatology*, vol. 55, no. 3, pp. 259–266, 2016.
- [11] J. Yakoob, W. Jafri, M. A. Beg et al., “Irritable bowel syndrome: is it associated with genotypes of *Blastocystis hominis*,” *Parasitology Research*, vol. 106, no. 5, pp. 1033–1038, 2010.
- [12] G. Shirvani, M. Fasihi-Harandi, O. Raiesi et al., “Prevalence and molecular subtyping of *Blastocystis* from patients with irritable bowel syndrome, inflammatory bowel disease and chronic urticaria in Iran,” *Acta Parasitologica*, vol. 65, no. 1, pp. 90–96, 2020.
- [13] M. Aykur, A. Camyar, B. G. Türk, A. Z. Sin, and H. Dagci, “Evaluation of association with subtypes and alleles of *Blastocystis* with chronic spontaneous urticaria,” *Acta Tropica*, vol. 231, Article ID 106455, 2022.
- [14] S. Viesy, Z. Rezaei, I. Pouladi, A. Mirzaei, and J. Abdi, “The prevalence of *Blastocystis* sp. and its relationship with gastrointestinal disorders and risk factors,” *Iranian Journal of Parasitology*, vol. 17, no. 1, pp. 90–95, 2022.
- [15] K. T. Moe, M. Singh, J. Howe et al., “Experimental *Blastocystis hominis* infection in laboratory mice,” *Parasitology Research*, vol. 83, no. 4, pp. 319–325, 1997.
- [16] S. S. R. Ajjampur and K. S. W. Tan, “Pathogenic mechanisms in *Blastocystis* spp.—interpreting results from *in vitro* and *in vivo* studies,” *Parasitology International*, vol. 65, no. 6, pp. 772–779, 2016.
- [17] M. K. Puthia, S. W. S. Sio, J. Lu, and K. S. W. Tan, “*Blastocystis ratti* Induces contact-independent apoptosis, F-actin rearrangement, and barrier function disruption in IEC-6 cells,” *Infection and Immunity*, vol. 74, no. 7, pp. 4114–4123, 2006.
- [18] J. A. Yason, Y. R. Liang, C. W. Png, Y. Zhang, and K. S. W. Tan, “Interactions between a pathogenic *Blastocystis* subtype and gut microbiota: *in vitro* and *in vivo* studies,” *Microbiome*, vol. 7, no. 1, Article ID 30, 2019.
- [19] S. Castañeda, M. Muñoz, X. Villamizar et al., “Microbiota characterization in *Blastocystis*-colonized and *Blastocystis*-free school-age children from Colombia,” *Parasites & Vectors*, vol. 13, no. 1, Article ID 521, 2020.
- [20] C. R. Stensvold, B. A. Sørland, R. P. K. D. Berg et al., “Stool microbiota diversity analysis of *Blastocystis*-positive and *Blastocystis*-negative individuals,” *Microorganisms*, vol. 10, no. 2, Article ID 326, 2022.
- [21] L. Deng and K. S. W. Tan, “Interactions between *Blastocystis* subtype ST4 and gut microbiota *in vitro*,” *Parasites & Vectors*, vol. 15, no. 1, Article ID 80, 2022.
- [22] L. Ma, H. Qiao, H. Wang et al., “Molecular prevalence and subtypes of *Blastocystis* sp. in primates in northern China,” *Transboundary and Emerging Diseases*, vol. 67, no. 6, pp. 2789–2796, 2020.
- [23] M. Chen, Y. Cui, C. Liu et al., “Characteristics of the microbiome in lung adenocarcinoma tissue from patients in Kunming city of southwestern China,” *Environmental Science and Pollution Research International*, vol. 30, no. 17, pp. 49992–50001, 2023.
- [24] J. Yakoob, W. Jafri, N. Jafri et al., “Irritable bowel syndrome: search of an etiology: role of *Blastocystis hominis*,” *The American Journal of Tropical Medicine and Hygiene*, vol. 70, no. 4, pp. 383–385, 2004.
- [25] H. S. Cheng, Y. L. Guo, and J. W. Shin, “Hematological effects of *Blastocystis hominis* infection in male foreign workers in Taiwan,” *Parasitology Research*, vol. 90, no. 1, pp. 48–51, 2003.
- [26] H. K. El Deeb, H. Salah-Eldin, and S. Khodeer, “*Blastocystis hominis* as a contributing risk factor for development of iron deficiency anemia in pregnant women,” *Parasitology Research*, vol. 110, no. 6, pp. 2167–2174, 2012.
- [27] O. K. Provance, E. S. Geanes, A. J. Lui et al., “Disrupting interferon-alpha and NF-kappaB crosstalk suppresses IFITM1 expression attenuating triple-negative breast cancer progression,” *Cancer Letters*, vol. 514, pp. 12–29, 2021.
- [28] A. Kelemen, I. Carmi, Á. Oszvald et al., “IFITM1 expression determines extracellular vesicle uptake in colorectal cancer,” *Cellular and Molecular Life Sciences*, vol. 78, no. 21–22, pp. 7009–7024, 2021.
- [29] I. Klymiuk, L. Kenner, T. Adler et al., “*In vivo* functional requirement of the mouse *Ifitm1* gene for germ cell development, interferon mediated immune response and somitogenesis,” *PLoS ONE*, vol. 7, no. 10, Article ID e44609, 2012.
- [30] C. Conrad, J. Benzel, K. Dorzweiler et al., “ADAM8 in invasive cancers: links to tumor progression, metastasis, and chemoresistance,” *Clinical Science*, vol. 133, no. 1, pp. 83–99, 2019.
- [31] Y. Dou, K. Zhu, Z. Sun, X. Geng, and Q. Fang, “Screening of disorders associated with osteosarcoma by integrated network analysis,” *Bioscience Reports*, vol. 39, no. 5, Article ID BSR20190235, 2019.
- [32] J. Hu, C. Han, J. Zhong et al., “Dynamic network biomarker of pre-exhausted CD8+ T cells contributed to T cell exhaustion in colorectal cancer,” *Frontiers in Immunology*, vol. 12, Article ID 691142, 2021.

- [33] C. D. Bingle and A. Vyakarnam, "Novel innate immune functions of the whey acidic protein family," *Trends in Immunology*, vol. 29, no. 9, pp. 444–453, 2008.
- [34] T. Nukiwa, T. Suzuki, T. Fukuhara, and T. Kikuchi, "Secretory leukocyte peptidase inhibitor and lung cancer," *Cancer Science*, vol. 99, no. 5, pp. 849–855, 2008.
- [35] M. G. O'Rand, E. E. Widgren, Z. Wang, and R. T. Richardson, "Eppin: an effective target for male contraception," *Molecular and Cellular Endocrinology*, vol. 250, no. 1-2, pp. 157–162, 2006.
- [36] M. G. O'Rand, E. E. Widgren, S. Beyler, and R. T. Richardson, "Inhibition of human sperm motility by contraceptive anti-eppin antibodies from infertile male monkeys: effect on cyclic adenosine Monophosphate1," *Biology of Reproduction*, vol. 80, no. 2, pp. 279–285, 2009.
- [37] S. Yenugu, R. T. Richardson, P. Sivashanmugam et al., "Antimicrobial activity of human EPPIN, an androgen-regulated, sperm-bound protein with a whey acidic protein Motif1," *Biology of Reproduction*, vol. 71, no. 5, pp. 1484–1490, 2004.
- [38] A. Indrieri, V. A. van Rahden, V. Tiranti et al., "Mutations in COX7B cause microphthalmia with linear skin lesions, an unconventional mitochondrial disease," *The American Journal of Human Genetics*, vol. 91, no. 5, pp. 942–949, 2012.
- [39] C. Rochette-Egly, S. Adam, M. Rossignol, J.-M. Egly, and P. Chambon, "Stimulation of RAR α activation function AF-1 through binding to the general transcription factor TFIID and phosphorylation by CDK7," *Cell*, vol. 90, no. 1, pp. 97–107, 1997.
- [40] L. Litov, P. Petkov, M. Rangelov et al., "Molecular mechanism of the anti-inflammatory action of heparin," *International Journal of Molecular Sciences*, vol. 22, no. 19, Article ID 10730, 2021.
- [41] S.-N. Ma, Z.-X. Mao, Y. Wu et al., "The anti-cancer properties of heparin and its derivatives: a review and prospect," *Cell Adhesion & Migration*, vol. 14, no. 1, pp. 118–128, 2020.
- [42] R. Schnoor, S. L. N. Maas, and M. L. D. Broekman, "Heparin in malignant glioma: review of preclinical studies and clinical results," *Journal of Neuro-Oncology*, vol. 124, no. 2, pp. 151–156, 2015.
- [43] D. A. Merida-de-Barros, S. P. Chaves, C. L. R. Belmiro, and J. L. M. Wanderley, "Leishmaniasis and glycosaminoglycans: a future therapeutic strategy?" *Parasites & Vectors*, vol. 11, no. 1, Article ID 536, 2018.
- [44] E. Lantero, J. Fernandes, C. R. Aláez-Versón et al., "Heparin administered to anopheles in membrane feeding assays blocks plasmodium development in the mosquito," *Biomolecules*, vol. 10, no. 8, Article ID 1136, 2020.
- [45] Z.-M. Zhang, X.-W. Zhang, Z.-Z. Zhao et al., "Synthesis, biological evaluation and molecular docking studies of 1,3,4-oxadiazole derivatives as potential immunosuppressive agents," *Bioorganic & Medicinal Chemistry*, vol. 20, no. 10, pp. 3359–3367, 2012.
- [46] R. Nagel, R. J. Traub, R. J. N. Allcock, M. M. S. Kwan, and H. Bielefeldt-Ohmann, "Comparison of faecal microbiota in *Blastocystis*-positive and *Blastocystis*-negative irritable bowel syndrome patients," *Microbiome*, vol. 4, no. 1, Article ID 47, 2016.
- [47] L. Deng, H. Tay, G. Peng, J. W. J. Lee, and K. S. W. Tan, "Prevalence and molecular subtyping of *Blastocystis* in patients with *Clostridium difficile* infection, Singapore," *Parasites & Vectors*, vol. 14, no. 1, Article ID 277, 2021.
- [48] C. M. Yañez, A. M. Hernández, A. M. Sandoval, M. A. M. Domínguez, S. A. Z. Muñiz, and J. O. G. Gómez, "Prevalence of *Blastocystis* and its association with *Firmicutes/Bacteroidetes* ratio in clinically healthy and metabolically ill subjects," *BMC Microbiology*, vol. 21, no. 1, Article ID 339, 2021.
- [49] D. Mariat, O. Firmesse, F. Levenez et al., "The *Firmicutes/Bacteroidetes* ratio of the human microbiota changes with age," *BMC Microbiology*, vol. 9, no. 1, Article ID 123, 2009.
- [50] A. Kodio, D. Coulibaly, A. K. Koné et al., "*Blastocystis* colonization is associated with increased diversity and altered gut bacterial communities in healthy malian children," *Microorganisms*, vol. 7, no. 12, Article ID 649, 2019.
- [51] C. Audebert, G. Even, A. Cian et al., "Colonization with the enteric protozoa *Blastocystis* is associated with increased diversity of human gut bacterial microbiota," *Scientific Reports*, vol. 6, no. 1, Article ID 25255, 2016.
- [52] M.-J. Kim, Y. J. Lee, T.-J. Kim, and E. J. Won, "Gut microbiome profiles in colonizations with the enteric protozoa *Blastocystis* in Korean populations," *Microorganisms*, vol. 10, no. 1, Article ID 34, 2022.